

INTERNATIONAL GEOSCIENCE &
REMOTE SENSING SYMPOSIUM
IGARSS '90

Vol.3

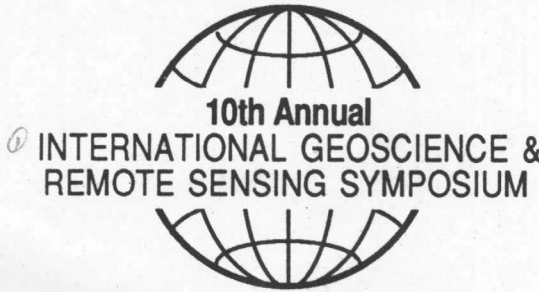
56-28083
I 61
1990(10)-3

REMOTE SENSING SCIENCE FOR THE NINETIES



IGARSS '90
WASHINGTON, D.C.

May 20-24



VOLUME III

The University of Maryland
College Park, Maryland

Library of Congress Number 89-82170
IEEE Catalog Number 90CH2825-8



Commission F

10th Annual

INTERNATIONAL GEOSCIENCE & REMOTE SENSING SYMPOSIUM IGARSS '90

VOLUME III

Copyright © 1990 by
THE INSTITUTE OF ELECTRICAL AND ELECTRONICS ENGINEERS, INC.
345 East 47 Street, New York, New York 10017

EDITOR: Ronnie Mills

Responsibility for the contents of the papers published in this digest rests upon the authors and not upon the IEEE or any of its members. All publication rights, including translations, are reserved by the IEEE and granted only on request. Abstracting is permitted with mention of source. Additional copies of the digest are available from:

The Institute of Electrical and Electronics Engineers, Inc.
445 Hoes Lane
Piscataway, New Jersey 08854

Order by IEEE Catalog Number 90CH2825-8
Library of Congress Catalog Card 89-82170

TABLE OF CONTENTS

VOLUME I

Welcome From the General Chairman	iii
IGARSS '90 Sponsors	iv
IGARSS '90 Organizing Committees	iv
Plenary Session	MA-1
<hr/>	
<i>Science of "Global Change" and a New Strategy for Earth Observations From Space</i> —Rasool, S.I.	3
<i>Data Needs in Global Change</i> —Webster, F.	5
<i>Remote Sensing of Precipitation From Space</i> —North, G.R.	7
<i>Cryospheric Data for Studies of Climatic Change</i> —Walsh, J.E., Parkinson, C.L.	9
Subsurface Methods	MP-1
<hr/>	
1. <i>Comparison of Whole- and Half-Space Models for TE Scattering From a Cylinder</i> —Shope, S.M., Wayland, J.R., Lee, D.O.	13
2. <i>Electromagnetic Detection of Buried Dielectric Targets</i> —Pedan, I.C., Schneider, J.B., Brew, J.	15
3. <i>Modelling of Well Logging Tools in a Multibed Environment With Invasions</i> —Chew, W.C., Nie, Z., Liu, Q.-H., Anderson, B.	19
4. <i>Induction Log Modeling Using Vertical Eigenstates</i> —Pai, D.M.	23
5. <i>Analysis of Electromagnetic Scattering From Buried Cylinders Using a Multifilament Current Model</i> —Meyouhas, Y., Levitan, Y.	27
6. <i>Modeling of the Subsurface Interface Radar</i> —Chew, W.C., Moghaddam, M., Yannakakis, E.	31
7. <i>Diffraction Tomography in Layered Background</i> —Pai, D.M.	33
8. <i>Applying a DSP to Seismic Monitoring</i> —Di Stefano, A., Mirabella, O., Sberna, G.	37

Contents

Poster: A Multi-DSP Based Monitoring Station for Realtime Detection and Evaluation of Earthquakes—Di Stefano, A., Mirabella, O.	41
Poster: Wave Propagation in Inhomogeneous Media: A Planewave Layer Interaction Method—Pai, D.M.	43

Radar Scattering

MP-2

1. Polarimetric Backscattering Characteristics of Three-Dimensional Random Targets: Multi-Polarization Scattering Coefficients Versus a Modified Mueller Matrix—Kobayashi, O., Hirosawa, H., Matsuzaka, Y.	49
2. High Frequency Scattering From Corrugated Stratified Cylinders—Sarabandi, K., Ulaby, F.T.	53
3. Power Spectrum of X-Band Backscatter From Wind-Influenced Vegetation—Narayanan, R.M., Doerr, D.W., Rundquist, D.C.	57
4. Multi-Frequency and Multi-Polarization Investigations of Microwave Backscatter From Vegetation and Bare Soil Under Dry and Wet Conditions—Schmullius, C.C.	59
5. Polarimetric Remote Sensing of an Anisotropic Half-Space Random Medium—Mudaliar, S., Lee, J.K.	61
6. Calibration of Polarimetric Radars Using In-Scene Reflectors—Yueh, S.H., Kong, J.A., Shin, R.T.	63
7. A CNTLM Spectral Analysis of Time Varying Lossy Dielectric Layers—Ko, W.L., Mittra, R.	65
8. General Time-Domain Solution for Fields Arising From a Dipole Above Lossless Ground—Nikoskinen, K.I., Lindell, I.V.	67

Clear Air Atmosphere Measurements/Propagation

MP-3

1. Studies of the Lower Marine Troposphere Using a Dual Frequency High Power Acoustic Sounder—Babin, S.M., Rowland, J.R., Miller, R.E.	71
2. Time Scale Refractive Index Measurements Within the Marine Evaporation Duct—Rowland, J.R., Meyer, J.H., Neues, M.R.	73
3. Fade Measurements and Statistics for Two Over-the-Water Propagation Links at C Band—Goldhirsh, J., Babin, S.M., Musiani, B.H., Gebo, N.E.	75
4. Analysis of Fade Characteristics for an Over-Water Microwave Link Path—Dockery, G.D.	77
5. Determination of Tropospheric Index Model Using Synoptic Meteorological Data—Diaz, W., Marcano, D.	79

6. Modeling and Measurement of the Spectral Properties of Atmospheric Oxygen Around 60 GHz —Liebe, H.J., Hufford, G., DeBolt, R.	83
7. Antenna Induced Clear Air Cross-Polarisation on Terrestrial LOS Links —Glover, I.A., McEwan, N.J.	85
8. Sensitivity of Troposcatter Communications to the Resolution of Radiosonde Data —Abdul-Jauwad, S.H., Halawani, T.U., Al-Khalidi, I.A., Harvey, W., Roberts, D.A., Meyer, J.H., Fahy, W.T.	87
Poster: A Single-Hop F2 Propagation Model for Frequencies Above 30 MHz and Path Distances Greater Than 4000 km —Rappaport, T.S., Campbell, R.L., Pocock, E.	91
Poster: Operation of Standard-A Earth Station Under Ionospheric Scintillation in Fixed Satellite Service —Fateem, M., Al-Majed S., Dawoud, M., El-Hennawy, M.	93
Poster: Olympus Propagation Experiment at Virginia Tech —Pratt, T., Stutzman, W.L., McKeeman, J.C.	95

Oceanography/Coastal I**MP-4**

1. Sediment Transport Pathways Along the Louisiana Coast —Rouse, L.J., Huh, O.K., Roberts, H.H., Rickman, D.	99
2. Remote Sensing Approach to Coastal Environmental Assessment and Management in and Around Vedaranyam, Tamil Nadu, India —Rajamanickam, G.V., Loveson, V.J., Singaram, N.	101
3. Landsat MSS Monitoring of Nile Delta Shoreline Changes —Blodget, H.W., Taylor, P.T., Roark, J.H.	105
4. Use of Satellite Spectral Data for Assessing Aquatic Macrophytes and Nutrient Levels in Lakes —Gao, T., Coleman, T.L.	109
5. Improving Quantitative Analysis of Inland Water Quality Using High Spectral Resolution Imaging and Non-imaging Data —Dekker, A.G., Malthus, T.J., Seyhan, E.	117
6. A Probability Model To Study Primary Productivity of Kentucky Lake —Lira, J., Marzolf, D., Marocchi, A., Naugle, B.	121
7. The Use of SPOT Data for Coastal Wave Analysis —Populus, J., Aristaghes, C.	125
Poster: Analysis of AVHRR Sea Surface Temperatures on Coastal Waters of Argentina Using Empirical Orthogonal Functions —Pettigiani, E., Karszenbaum, H., Schultze, M.M., Mejail, M., Segal, S.	129

Contents

Microwave Models/Measurements I	MP-5
<hr/>	
1. <i>Nimbus-7 37 GHz Observations of Seasonal and Interannual Variations of South American Wetlands, 1979-1986</i> —Choudhury, B.J.	133
2. <i>A Canopy Scattering Model and Its Applications to a Deciduous Forest</i> —Karam, M.A., Fung, A.K.	137
3. <i>Mimics II: Radiative Transfer Modeling of Discontinuous Tree Canopies at Microwave Frequencies</i> —McDonald, K.C., Ulaby, F.T.	141
4. <i>Microwave Signatures for Snow Covered First-Year Sea Ice</i> —West, R., Winebrenner, D.P., Tsang, L.	143
5. <i>Quantitative Estimation of Standing Biomass From L-Band Multipolarization Data</i> —Paris, J.F., Ustin, S.L.	147
6. <i>Polarimetric Radar Measurement of Forested Areas: 1989 Mt. Shasta Area Experiment</i> —Durden, S.L., Klein, J.D., Zebker, H.A., van Zyl, J.J.	151
7. <i>Experimental Study of Multiple Bounces in Radar Scattering From Trees</i> —Racette, P.E., Forster, R.R., Moore, R.K.	153
8. <i>Statistical Modeling for Polarimetric Remote Sensing of Earth Terrain</i> —Yueh, S.H., Kong, J.A., Shin, R.T., Zebker, H.A.	157
Poster: <i>Pade Approximant Scattering From a Deciduous Forest</i> —Karam, M.A., Fung, A.K.	161
Corrections/Atmospheric Effects	MP-6
<hr/>	
1. <i>Radiometric Rectification of Multi-Date, Multi-Sensor Satellite Images</i> —Hall, F.G., Strelak, D.E., Goetz, S.J., Nickeson, J.E.	165
2. <i>Atmospheric Correction Based on the CZCS-Multicolour Data</i> —Mukai, S., Sano, I., Takemata, K., Masuda, K., Sugimori, Y., Fukushima, H., Miyata, T.	169
3. <i>Atmospheric Corrections Based on Texture Features Reduction. Applications to AVHRR/NOAA and Simulated MODIS Data</i> —Tanre, D., Holben, B., Kaufman, Y., Kalb, G.	173
4. <i>Application of Lowtran 7 as an Atmospheric Correction to Airborne Visible/Infrared Imaging Spectrometer (AVIRIS) Data</i> —van den Bosch, J.M., Alley, R.E.	175
5. <i>Application of Heterogenous Scene Models to Retrieval of Land Surface and Atmospheric Optical Properties From Space</i> —Martonchik, J.V., Diner, D.J., Danielson, E.D., Bruegge, C.J.	179
6. <i>Simulation of Atmospheric and Topographic Effects in Remote Sensing From Space</i> —Kagiwada, H.H., Ueno, S., Kawata, Y.	183

Contents

7. Second Simulation of the Satellite Signal in the Solar Spectrum-6S Code— Tanre, D., Deuze, J.L., Herman, M., Santer, R., Vermonte, E.	187
8. Effects of the Atmosphere and Surface Emissivity on the Thermal Infrared Spectral Signature Measured From MODIS-N— Wan, Z., Dozier, J.	189
Poster: Optical Atmospheric Effects in High Resolution Satellite Imagery To Evaluate Quantitatively and Qualitatively Air Pollution Plumes; Two Case Studies: Toulouse (France) and Athens (Greece)— Sifakis, N.I., Lambiris, K., Aumonier, F.	193

Passive Microwave Systems **MP-7**

1. A Performant Radiometer Between 110 and 190 GHz for Temperature and Water Vapour Sounding of the Atmosphere: Prospective Attractive Airborne Campaigns— Abba, P., Beaudin, G., Deschamps, A., Encrenaz, P., Gheudin, M., Jegou, J.R., Prigent, C., Ruffie G.	197
2. DMSP SSM/I: Current Status— Hollinger, J.P.	201
3. TOPEX/POSEIDON Microwave Radiometer Post-Launch Ground Based Calibration/Validation— Ruf, C.S., Keihm, S.	203
4. Microwave Remote Sensing at the JRC— Sieber, A.J., Klersy, R.	207
5. Objectives and Overall Design of the European Microwave Signature Laboratory— Sieber, A.J., Nesti, G.	213

Remote Sensing in Tropical Forests **MP-8**

1. Estimating Brazilian Amazon Deforestation Using TM and the Influence of Deforestation on the Local Biota Using GIS— Tucker, C.J., Grant, T., Newcomb, W.W.	221
2. NOAA/AVHRR as a Data Source for a Tropical Forest GIS— Cross, A.	223
3. Mapping and Monitoring the Forest Boundary of Central Africa— Kendall, J.D., Justice, C.	227
4. GIS and Remotely Sensed Data for Monitoring Tropical Forests— Otoo, J.E.	229
5. Establishing the Okapi Rain Forest Reserve: Avoiding Human Land-Use Conflicts Using Satellite Image Analysis— Wilkie, D.S.	233
6. The Applicability of the AVHRR To Monitor Forest Conversion in Kalimantan, Indonesia— Malingreau, J.P., Laporte, N.	237

Contents

Moderate Resolution Land Analysis	MP-9
<hr/>	
1. <i>A Low-Cost Receiving Station for Environmental Studies</i> —Baumgartner, M.F., Fuhrer, M.	241
2. <i>Geometrical Considerations in the Determination of Effective Parameters From SPOT HRV Data To Be Applied in Agroclimatological Models With NOAA AVHRR Data</i> —Moreno, J., Gandia, S., Melia, J.	245
3. <i>Estimation of the Broadband Planetary Albedo From Narrowband NOAA Satellite Observations</i> —Jacobowitz, H., Gruber, A.	249
4. <i>Effects of Atmospheric Composition and Viewing Geometry on MODIS and AVHRR Normalized Difference Vegetation Indices</i> —Hoyt, D.V.	253
5. <i>AVHRR Compositing Using NDVI and Thermal Channel Data</i> —D'Iorio, M.A., Cihlar, J., Mullins, D.W.	257
6. <i>Satellite-Derived Indices for Monitoring Global Phytopl climatology</i> —Gallo, K.P., Brown, J.F.	261
7. <i>Mapping Regional Forest Evapotranspiration and Photosynthesis by Coupling Satellite Data With Ecosystem Simulation</i> —Running, S.W., Coughlan, J.C., Peterson, D.L., Band, L.E.	265
Poster: <i>Relationships Between Surface Parameters and NDVI in the U.S.</i> —Levine, E., Kerber, A., Nelson, R.	269
 Signal Processing Noise and Calibration	MP-10
<hr/>	
1. <i>Extending Relational Algebra To Manipulate Preprocessed Remote Sensing Images</i> —Xiao, Q., Raafat, H.	273
2. <i>Application of the Walsh-Hadamard Transform to Satellite Radar Altimetry</i> —Arambepola, B., Bestwick, D.J., Partington, K.C.	277
3. <i>Unbiased Minimum Variance Estimation of Correlation Functions of Random Signals</i> —Chi, C.-Y., Chen, W.-T.	281
4. <i>Adaptive Size Median Filter by Using Local Entropy</i> —Zhou, W., Blais, J.A.R.	285
5. <i>Application of a Station Filtering Algorithm for Removal of Scan-Line Noise From Landsat TM Data</i> —Jones, J.M., Naugle, B.I.	289
6. <i>Analog-to-Digital-to-Analog Conversions: An Analysis of Improvements and Degradations in LFC Color Infrared Imagery</i> —Heric, M., Guernsey, C.	293
7. <i>Combined Use of Parametric Spectrum Estimation and Frost-Algorithm for Radar Speckle Filtering</i> —Quelle, H.-Ch., Boucher, J.-M.	295
Poster: <i>Maximum-Likelihood Impulse Response Estimation With Impulsive-Gaussian Noise Corrupted Data</i> —Chi, C.-Y., Kung, J.-Y.	299

Poster: Satellite Photographic Mapping With Computer Optical Differential Projection Transformation System—Mao, C., Li, H., Xia, F.	301
<hr/>	
SAR Geometry and SNR Improvement	MP-11
<hr/>	
1. Parameters for Geometric Fidelity of Geocoded SAR Products—Schreier, G., Raggam, J., Strobl, D.	305
2. Automated Matching of Real and Simulated SAR Imagery for Geometric Correction—Kimura, H., Iijima, T.	309
3. SAR Object Detection With Fractal Terrain Models—Harger, R.O.	313
4. A Comparison of the Detection Performances Obtained With a Fully Polarized SAR and a Dual Polarized SAR (HH, VV)—Nasr, J.-M., Fernin, P.	317
5. Improved Multi-Look Techniques Applied to SAR and SCANSAR Imagery—Moreira, A.	321
6. Progress in Polarimetric SAR Processing, Calibration, and Analysis at the Defense Research Establishment Ottawa—Rey, M.T., Saper, R., Armour, B., Ehrismann, J.	325
Poster: Innovative Algorithms for SAR to Optical Image Registration—Curlander, J., Kober, W.	329
Poster: SAR Bistatic Scenarios in Space Exploration Missions—Dendal, D., Marchand, J.L.	333
<hr/>	
Image Analysis	MP-12
<hr/>	
1. Polarization Signatures of Frozen and Thawed Forests of Varying Biomass—Kwok, R., Way, J., Rignot, E., Freeman, A., Holt, J.	337
2. A Facility To Measure Both Pattern and Process in Global Change—Goetz, A.F.H.	341
3. Spectral Decomposition of Sea Surface Reflected Radiance—Pilorz, S.H., Davis, C.O.	345
4. A Fast Multistage Gaussian Maximum Likelihood Classifier—Lee, C., Landgrebe, D.A.	349
5. nPDF-An Algorithm for Mapping n-Dimensional Probability Density Functions for Remotely Sensed Data—Cetin, H.	353
6. Displaying Multispectral Images on Video Terminals in RGB Color—Lin, Q., Allebach, J.	357
7. LOSSI Compression Techniques for Hyperspectral Imagery—Tse, Y.-T., Kiang, S.-Z., Chiu, C.-Y., Baker, R.L.	361

Contents

Inversion and Signal Processing for Geoscience	TA-1
<hr/>	
1. <i>Simultaneous Phase and Group Slowness Estimation From Dispersive Wave-forms</i> —Hsu, K., Esmersoy, C., Marzetta, T.L.	367
2. <i>Velocity Filters for Multiple Interferences in Two Dimensional Geophysical Data</i> —Chen, C.-M., Simaan, M.	371
3. <i>Joint Inversion of Magnetic and Potential Data for Subsurface Resistivity</i> —Sezginer, A.	375
4. <i>Reconstruction of Permittivity Distribution Using the Born Iterative and Distorted Born Iterative Methods for Geophysical Applications</i> —Wang, Y.M., Chew, W.C.	379
5. <i>Inversion With Variational Constraints</i> —Berryman, J.G.	383
6. <i>Diffraction Tomography for Geophysical Imaging in Hydrocarbon Research</i> —Justice, J., Vassilion, A.A.	387
 Surface Scattering	TA-2
<hr/>	
1. <i>Numerical Point Target Simulation of Radar Backscatter From Random Surface</i> —Swart, P.J.F., Sliedregt, M.v., Snoeij, P.	393
2. <i>A One-Scale Reflection Model for Ocean Imaging by SAR</i> —Milman, A.S.	397
3. <i>A Scattering Correction Model for the Inversion of Microwave Radiometric Measurements of the Sea Surface and the Atmosphere</i> —Guissard, A., Sobieski, P., Laloux, A., Baufays, C.	401
4. <i>An Iterative Approach to Surface Scattering Simulation</i> —Chen, K.S., Fung, A.K.	405
5. <i>Reconsideration of the SAR Modulation Transfer Function for the Imaging of Ocean Surface Waves</i> —Monaldo, F.	409
6. <i>Inversion of Synthetic Aperture Radar Data for Surface Scatterer</i> —Won, J.S., Moon, W.M.	413
7. <i>Modeling the Presence of Ocean Wave Group Peaks in the Dual Frequency Doppler Spectrum</i> —Jacobsen, S., Eltoft, T.	417
 Measurements of Rain From Space and Earth Platforms	TA-3
<hr/>	
1. <i>Scattering From Clouds and Rain: Requirements for a Spaceborne Radar</i> —Crane, R.	423

Contents

2. Spaceborne Radar for Rain and Cloud Measurements: A Conceptual Design— Im, E., Kellogg, K.	425
3. Analysis of Airborne Radar and Radiometer Rain Measurements and Their Relationship to Spaceborne Observations— Meneghini, R., Kozu, T., Kumagai, H., Boncyk, W.C.	429
4. Analysis of Cross-Beam Resolution Effects in Rainfall Rate Profile Retrieval From a Spaceborne Radar— Amayenc, P., Marzoug, M., Testud, J.	433
5. Error Model for Combined Radar and Radiometer Measurements of Rain From Space— Wilheit, T.T.	437
6. The Estimation of Convective Rain From Space by Area Integrals and Associated Ground Truth— Atlas, D.	439
7. Time Series Analysis of Rainfall in Alexandria, Egypt— Abu Hashem, A.A., Abu-El Hassan, A., Kheirallah, H.N.	441

Oceanography/Coastal II TA-4

1. Application of AVHRR Satellite Data to the Study of Temperature, Sediment and Pigment Distributions in Coastal Waters of Argentina— Frulla, L., Gugliardini, D.A., Karszenbaum, H., Schultze, M.M., Milovich, J.A.	447
2. Remote Sensing Observations of the Tay Estuary, Scotland— Ferrier, G., Anderson, J.M.	449
3. Preliminary Evaluation of a Multi-Channel SAR Data Set for a Mid-Atlantic Coastal Marsh— Ott, J.S., Kasischke, E.S., French, N.H., Gross, M., Klemas, V.	453
4. Remote Detection of Stratification on Georges Bank— Bisagni, J.J.	457
5. APEX Predator Fish Distributions, Bathymetry and Sea Surface Temperature Fronts off the Northeast United States— Strout, G.A., Christenson, D.	463
6. Active and Passive Microwave Measurements of Natural Surface Slicks During SLIX '90— Onstott, R.G., Shuchman, R.A., Gaboury, S., Lyzenga, D.R.	467
Poster: Use of Multispectral Video Data for Water Quality Evaluation in Hudson/Rarita Estuary— Bagheri, S., Islam, K.R.	469
Poster: A Practical, Multi-Gbyte GIS/Database for the Coast of Louisiana— Rickman, D., Huh, O., Clark, R., Rouse, L.	471

Microwave Models/Measurements II TA-5

1. Microwave Polarimetric Scattering Measurements of Rough Surfaces— Ulaby, F.T., Sarabandi, K.	475
--	-----

Contents

2. Comparison of Integral Equation Predictions and Experimental Backscatter Measurements From Random Conducting Rough Surfaces—	
Nance, C.E., Fung, A.K., Bredow, J.W.	477
3. Radar Sensitivity to Forest Stand Parameters—	Lang, R.H., Chauhan, N.
	481
4. Polarimetric Radar Backscatter Modeling for Discontinuous Canopies—	
Sun, G., Simonett, D.S.	483
5. A Multiple-Polarization Layered Radar Model for Mangal Forest—	Wang, Y.,
Simonett, D.S., Imhoff, M.L.	487
6. Principles of a High Resolution Forest Imaging Model for SAR—	Miller, R.J.,
Brown, L.M.J., Sieber, A.J.	491
7. Experimental Analysis of Linearizing Approximations in Inverse Scattering—	
Schindel, R.F., Blanchard, A.J.	495
8. Ground Data Verification—	Churchill, P.N., Miller, R.J.
	499
Poster: Dielectric Properties of Two Western Coniferous Tree Species—	Hess, L.,
Simonett, D.S.	503

Sensor Calibration	TA-6
---------------------------	-------------

1. Irradiance-Based Calibration of Imaging Sensors—	Biggar, S.F., Santer, R.P.,
Slater, P.N.	507
2. Inflight Calibration of the NOAA-AVHRR Visible and Near IR Channels—	
Kaufman, Y.J., Holben, B.N., Kendall, J.D., Mekler, Y.	511
3. Radiometric Calibration of Aircraft and Satellite Sensors at White Sands, NM—	Markham, B.L., Irons, J.R., Deering, D.W., Halthore, R.N., Irish, R.R., Jacksons, R.D., Moran, M.S., Biggar, S.F., Gellman, D.I., Grant, B.G., Palmer, J.M., Slater, P.N.
	515
4. Self-Calibration of Doppler Weather Radars for Performance Improvement—	
Mahapatra, P.R., Zrnic', D.S.	519

Wind Measurements	TA-7
--------------------------	-------------

1. Measurements of Vertical Wind by the Flatland Radar—	VanZandt, T.E.,
Green, J.L., Clark, W.L., Gage, K.S., Warnock, J.M., Nastrom, G.D.	525
2. Recent Developments in the Application of Wind-Profiling Doppler Radars to Tropical Dynamics and Climate Research—	Gage, K.S.
	527
3. Wind Profiler Observations of Midtropospheric Cyclogenesis—	Zamora, R.J.,
May, P.T.	529

Contents

4. Evaluating the Performance of the First Wind Profiler of the New NOAA Demonstration Network —Wuertz, D.B., Weber, B.L., Strauch, R.G., Merritt, D.A., Moran, K.P., Law, D.C., van de Kamp, D., Chadwick, R.B., Ackley, M.H., Barth, M.F., Abshire, N.L., Miller, P.A., Schlatter, T.W.	533
5. Analysis of Comparative Wind Profiler and Radiosonde Measurements —Thomson, D.W., Williams, S.R.	537
6. Evaluation of Cloud Motion Vectors —Thomasell, A.	541
7. Model-Based Wind Estimation Using Seasat Scatterometer Measurements —Long, D.G.	545
Poster: Determination of Weather Attractors Using Atmospheric Remote Sensing Systems —Thomson, D.W., Henderson, H.W.	549
Poster: Identifiability in Wind Estimation From Scatterometer Measurements —Long, D.G., Mendel, J.M.	553

Terrestrial Ecology

TA-8

1. Modeling of Terrestrial Ecosystems With Remotely Sensed Inputs —Schimel, D., Wessman, C., Parton, W., Curtiss, B., Knapp, A., Seastedt, T., Goetz, A.	557
2. Models for Remote Sensing of Primary Production at the Regional and Global Scales —Prince, S.D., Goward S.N., Dye, D.G., Daughtry, C.S.T.	559
3. The Effect of Water Content and Intact Cuticle on the Estimation of Nitrogen, Lignin and Cellulose Content of Forest Foliage Samples —Martin, M., Aber, J.	563
4. An Airborne Perspective on Vegetation Phenology From the Analysis of AVIRIS Data Sets Over the Jasper Ridge Biological Preserve —Miller, J.R., Elvidge, C.D., Rock, B.N., Freemantle, J.R.	565
5. Spectral Characterization of Phenological Change and Insect-Related Damage in Sugar Maple —Vogelmann, J.E.	569
6. Swamp Forest Differentiation With Multipolarized and Multiple Incidence Angle L-Band Radar Data —Hussin, Y.A., Hoffer, R.M.	573
7. Using Airborne Laser Profiler Data To Determine Shrub Cover in a South Texas Rangeland —Ritchie, J.C., Davis, R., Everitt, J.H.	577
Poster: Reflectance of Visible and Infrared Radiation From Pine Foliage as Affected by Ecotomycorrhizae —Cibula, W.G., Carter, G.A.	581
Poster: The Potential for Estimating Biogeochemical Parameters From Imaging Spectrometry Data for Forest Ecosystem Modeling —Curtiss, B., Ustin, S.L.	583

Contents

Agriculture	TA-9
<hr/>	
1. <i>Estimation of APAR Values From AVHRR NDVI for Regional Crop Yield Assessment in West Africa</i> —Bartholome, E.	587
2. <i>Remote Sensing of Droughts</i> —Kogan, F.N.	591
3. <i>Data Treatment for Agricultural Statistics</i> —Stakenborg, J.	595
4. <i>Comparison of Sensors for Corn and Soybean Planted Area Estimation</i> —Bellow, M.E.	599
5. <i>Spectral Reflectance Characteristics of Wheat Residue</i> —Major, D.J., Larney, F.J., Lindwall, C.W.	603
6. <i>Remote Sensor Comparison for Crop Area Estimation Using Multi-temporal Data</i> —Allen, J.D.	609
7. <i>Mapping Winter Grazing Areas for Reindeer in Finnmark Country, Northern Norway, Using Landsat 5-TM Data</i> —Johansen, B., Tommervik, H.	613
8. <i>Identification and Monitoring of Anopheles Freeborni Habitats in Northern California</i> —Wood, B., Washino, R., Pitcairn, M., Rejmankova, E., Hibbard, K., Beck, L., Whitney, S., Salute, J.	617
Poster: <i>Predicting Mosquito Populations in California Rice Fields</i> —Hibbard, K., Washino, R., Wood, B., Pitcairn, M., Rejmankova, E., Salute, J., Beck, L.	621
Geometric Registration, Rectification, and Resampling	TA-10
<hr/>	
1. <i>Registration Accuracy for Noisy Images</i> —Frankot, R.T.	625
2. <i>Accurate Determination of Ground Control Points for SPOT Image Rectification</i> —Zhou, G., Mausel, P.W., Brooks, W.D.	629
3. <i>A Multiresolution Approach for Registration of a SPOT Image and a SAR Image</i> —Wu, Y., Maitre, H.	635
4. <i>Residual Focusing of SAR Images</i> —Monti-Guarnieri, A., Prati, C., Damonti, E.	639
5. <i>Edge Detection and Hough Transform Techniques Applied to High-Relief SAR Imagery for Automatic Registration</i> —Fernin, Ph., Nasr, J.-M.	643
6. <i>The Effects of the Application of Smoothing and Orthogonal Transforms to SPOT and TM Data on Regression Based Crop Acreage Estimates</i> —Winings, S.B., Ozga, M., Stakenborg, J.	647
7. <i>An Image Connection of NOAA AVHRR Data in Plural Orbits</i> —Nakayama, Y., Tanaka, S.	651
Poster: <i>Use of an Airborne GPS for Geometric Correction of Scanner Imagery</i> —Rickman, D.	655

Contents

- Poster: Geometric Rectification of High Resolution Airborne Multispectral Data—Lingsch, S.C., Kalcic, M.T.** 657

Subsurface Sediment Geology TP-1

- 1. A Modelling and Estimation Approach for the Extraction of the Geophysical Parameters of Marine Deposits From Acoustic Measurements—Peirlinckx, L., Masyn, S., Van Biesen, L.** 661
- 2. A New Seismo-Acoustic Probe for Seabed Measurements—Owen, T., Rossfelder, A.M.** 669
- 3. A Knowledge Based Measurement as a Link Between the Engineering and Geological Aspects in the Construction of a Subbottom Mapping Device—Masyn, S., Peirlinckx, L., Van Biesen, L., Faas, R., Wartel, S.** 671
- 4. Soil-Type, Identification Using Active Mid-Infrared Reflectance Characteristics—Narayanan, R.M., Green, S.E., Alexander, D.R.** 673
- 5. Determining Organic and Mineral Sediment Distributions for a Shallow Coastal Environment Using Airborne Electromagnetic Profiler Data—Pelletier, R.E., Wu, S.T.** 675
- 6. Submarine Bottom Topography Imaging Using Ka- and L-Band Radar: A Discussion Based on Latest Theoretical and Experimental Results—Hennings, I.** 679
- 7. The Atchafalaya-Chenier Plain Sedimentary System—Huh, O.K., Roberts, H.H., Rouse, L.J., Rickman, D.** 683
- 8. Mapping of Soil Material in SW Messinia (Greece) Using SPOT-HRV Data—Brackman, P., Goossens, R.** 685

Radar Modulation Mechanisms TP-2

- 1. Automatic Ship Image Extraction From Synthetic Aperture Radar Imagery—Klepko, R.** 691
- 2. Frequency Dependence of Electromagnetic Bias in Sea Surface Range Measurements—Walsh, E.J., Jackson, F.C., Hines, D.E., Piazza, C., Hevizi, L.G., McIntosh, R.E., McLaughlin, D.J., Swift, R.N., Scott, J.F., Yungel, J.K., Frederick, E.B.** 695
- 3. Altimeter Response to Nonlinear Surface Wavefields—Poitevin, J., Ramamonjiarisoa, A., Kharif, C.** 699
- 4. Nonlinear Effects in Many Look SAR Imagery of the Ocean—Jensen, J.R.** 703
- 5. NORCSEX '88: A Pre-Launch ERS-1 Satellite Study of SAR Imaging Capabilities of Upper Ocean Circulation Features and Wind Fronts—Johannessen, J.A., Shuchman, R.A., Johannessen, O.M.** 707

Contents

6. Observations of Large Scale Variations in Sea Surface Topography From Space —Koblinsky, C.J.	711
7. Use of High Frequency Radar for the Measurement of Ocean Surface Currents —Fernandez, D.M., Vesecky, J.F., Roughgarden, J.M., Teague, C.C., Napolitano, D.J.	715

Weather Radar Research and Applications TP-3

1. Retrieval of Flow and Thermodynamic Fields From Single Doppler Radar for Prediction Model Initialization —Lilly, D.K., Gal-Chen, T., Sun, J., Liou, Y.C.	721
2. NEXRAD and the Operational Doppler Weather Radar for the 1990s and Beyond —Alberty, R.L., Crum, T.D.	725
3. Clutter Rejection for Doppler Weather Radars With Staggered Pulses —Banjanin, Z., Zrnic', D.S.	729
4. Rapid Scan Doppler Weather Radar Measurements —Girardin, J., Baudin, F., Testud, J.	733
5. Radar Observation of a Periodic Atmospheric Wave Train —Mahapatra, P.R., Doviak, R.J., Zrnic', D.S.	737
6. An Algorithm for Wind Reconstruction From Scatterometer Data —Bartoloni, A., Zirilli, F.	741
7. Terrain Doppler Weather Radar Gust Front Algorithm —Stumpf, G.J.	743

Radar Ocean Scattering I TP-4

1. Real-Time Airborne Real Aperture Radar: The System and Its Applications —Keller, W.C., Askari, F.	749
2. The Phelps Bank Revisited: A Comparison Between Observations and Models —Askari, F., Chubb, S.R., Keller, W.C., Valenzuela, G.R.	751
3. Global Wave Forecasting Using Spaceborne SAR: Implication From SEASAT, SIR-B, and LEWEX —Beal, R.	753
4. Probing the Ocean Surface With Microwave Radar —Thompson, D.R.	755
5. Dependence of Radar Backscatter on the Energetics of the Air-Sea Interface —Colton, M.C.	757
6. Wind Regimes for Scatterometer Response From Wind-Generated Seas —Bliven, L., Wanninkhof, R., Giovanangeli, J.P., Chapron, B.	761